NJC

PAPER

View Article Online
View Journal | View Issue

Cite this: *New J. Chem.*, 2015, 39, 1883

# The effect of 4-halogenobenzoate ligands on luminescent and structural properties of lanthanide complexes: experimental and theoretical approaches†

Jorge H. S. K. Monteiro,[a] Ana de Bettencourt-Dias,[b] Italo O. Mazali[a] and Fernando A. Sigoli*[a]

Received (in Victoria, Australia) 30th September 2014,
Accepted 16th December 2014

DOI: 10.1039/c4nj01701c

www.rsc.org/njc

The ligands 4-fluorobenzoate (4-fba), 4-chlorobenzoate (4-cba), 4-bromobenzoate (4-bba) and 4-iodobenzoate (4-iba) were chosen in order to synthesize europium(III), gadolinium(III) and terbium(III) complexes and compare the effect of halogens on their physical chemistry and luminescent properties. The homobimetallic complex $[Eu(4\text{-iba})_3(H_2O)(dmf)]_2$ crystallizes in the monoclinic $P2_1/c$ space group with unit cell parameters $a$ = 8.3987(9) Å, $b$ = 25.314(3) Å, $c$ = 14.1255(17) Å, and $\beta$ = 105.347(2)°. FTIR spectroscopy indicates that the bidentate bridging mode of the carboxylato ligand was present in all complexes while bidentate chelate and a mixture of bidentate bridging and chelate modes were also found. According to emission spectra profiles and the Judd–Ofelt parameters the halogen of ligand molecules modifies the chemical environment symmetry around the europium(III) ion in their respective complexes. The complexes $[Eu(4\text{-fba})_3(H_2O)_2]$ and $[Eu(4\text{-iba})_3(H_2O)_2]$ have the highest symmetry around the europium(III) while the complexes $[Eu(4\text{-cba})_3]\cdot 2H_2O$, $[Eu(4\text{-bba})_3]\cdot 5/2H_2O$ and $[Eu(4\text{-iba})_3(H_2O)(dmf)]_2$ have the lowest. The different halogens at the *para* position do not change the covalence degree of Eu–O bonds significantly, however they play a role in the ligand to metal charge transfer energies. The highest non-radiative energy transfer rates from ligand to europium(III) were found for the complexes $[Eu(4\text{-cba})_3]\cdot 2H_2O$ and $[Eu(4\text{-bba})_3]\cdot 5/2H_2O$.

## Introduction

The luminescent properties of lanthanide(III) compounds, due to the 4f–4f transitions, have been applied in several fields such as illumination, displays, OLEDs, sensors, luminescent markers, *etc.*[1–3] A strategy to increase the emission intensity of the lanthanides(III) is the coordination of organic chromophores to them. The absorbed energy by the ligand may be transferred from the ligand to the lanthanide *via* excited singlet, charge transfer states or triplet levels, the triplet → lanthanide(III) normally being the most efficient one due to the energy resonance and selection rules imposed by lanthanide ions.[2,4] Carboxylate ligands are interesting due to their spectroscopic properties, usually high energy of triplet level and they show several coordination modes, such as bidentate bridging, bidentate chelate, monodentate, *etc.*[5] Li and co-workers[6] obtained a dimeric terbium(III) complex using the ligand 2-fluorobenzoate (2-fba). Xu and co-workers[7] obtained a similar dimer of europium(III) using the ligands 4-fluorobenzoate (4-fba) and phenanthroline. Zhang[8] showed an example of a dimer of dysprosium(III) with the ligands 4-chlorobenzoate (4-cba) and phenanthroline. Some examples of dimers of dysprosium(III) complexes was also shown by Li and co-workers[9] using the ligands 2-chlorobenzoate (2-cba) and bipyridine or 2-bromobenzoate (2-bba) and phenanthroline. Zhang and co-workers[10] showed an example of a dimer for a samarium(III) complex with the 4-bromobenzoate (4-bba) and the bipyridine as the auxiliary ligand. Li and co-workers[11] reported the synthesis, single crystal structure and some photophysical properties of europium(III) complexes with the ligands 2-iodobenzoate (2-iba) and water or phenanthroline or 2,2′-bipyridine.

In all research results cited above, the syntheses of complexes, single crystal structures and different coordination modes are highlighted for complexes containing ligand derivatives of benzoic acid.[6–11] The presence of different halogens

[a] *Department of Inorganic Chemistry, Institute of Chemistry, University of Campinas, Campinas, São Paulo, Brazil. E-mail: fsigoli@iqm.unicamp.br*
[b] *Department of Chemistry, University of Nevada, Reno, NV 89557, USA*

† Electronic supplementary information (ESI) available: Elemental analysis, TGA and DTA curves, FT-IR spectra, UV-Vis absorption spectra, time resolved phosphorescence spectra of the gadolinium(III) complexes, emission decay curves, ground state geometry and charge factors ($g$) and polarizabilities ($\alpha$). CCDC 1024660. For ESI and crystallographic data in CIF or other electronic format see DOI: 10.1039/c4nj01701c

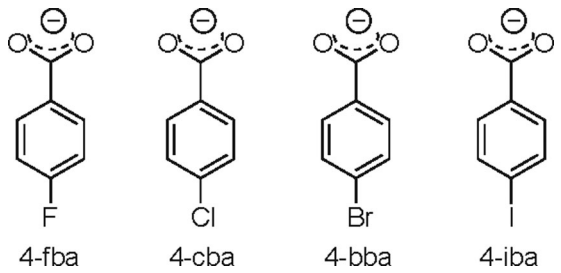


Fig. 1 Molecular structures of the ligands: 4-fluorbenzoate (4-fba), 4-chlorobenzoate (4-cba), 4-bromobenzoate (4-bba) and 4-iodobenzoate (4-iba).

(F, Cl, Br or I) may change some physical chemistry properties of the lanthanides(III) complexes, such as (i) solubility in polar solvents due to the presence of the fluorine atom in the ligand structure; (ii) changes in the Eu–O covalence degree upon addition of the chlorine atom in the ligand structure, as reported by Malta and co-workers;[12] (iii) increase in the inter-system crossing (ISC) efficiency due to the presence of the iodine atom in the ligand structure as reported by Lower and El-Sayed;[13] (iv) the triplet level energy and (v) the energy of ligand to metal charge transfer states (LMCT) of europium(III) complexes.

The understanding of the correlation between the ligand molecular structure and the energy transfer processes from ligand to lanthanide(III) ions provides a good background for planning future luminophores with high emission quantum yields. Therefore, the main goal of this work is the evaluation of the halogen effect under the structural and photophysical properties of a series of 4-halogenobenzoate lanthanide(III) complexes. The ligands chosen for this purpose are shown in Fig. 1.

The ligands shown in Fig. 1 allow a good comparison of the halogen effect on the photophysical properties of the lanthanide(III) complexes due to a similar coordination unit (the carboxylate group) and molecular/crystalline structures. In order to compare the changes in the molecular and crystalline structures and photophysical properties of the lanthanide(III) complexes, results from single crystal X-ray diffraction, TGA, FT-IR, DRS, luminescence spectroscopy and ground state geometries and energy transfers theoretical calculations will be presented in this work.

## Experimental section

### General procedure for $LnCl_3$ (Ln = $Eu^{3+}$, $Gd^{3+}$ or $Tb^{3+}$)

All commercially obtained reagents were of analytical grade and were used as received. The lanthanide(III) chlorides, $LnCl_3$ (Ln = $Eu^{3+}$, $Gd^{3+}$ or $Tb^{3+}$), were obtained by the addition of hydrochloric acid into a lanthanide oxide aqueous suspension. After complete dissolution of the oxides the pH of the solution was adjusted to $\sim$4 with diluted ammonium hydroxide aqueous solution (0.1 mol $L^{-1}$). In the case of terbium oxide a few drops of hydrogen peroxide (29% wt/vol) were added in order to reduce terbium(IV) to terbium(III).

### General procedure for $[Ln(L)_3(H_2O)_x]\cdot(H_2O)_y$ synthesis[14]

Sodium hydroxide was added to aqueous suspensions of ligands in a 1 : 1 ($L:OH^-$) molar ratio and stirred for 30 min at 80 °C. The aqueous solutions of deprotonated ligands were added to aqueous $LnCl_3$ solution in a 1 : 3 molar ratio (Ln : L). White precipitates were formed and the suspensions were kept under stirring at 80 °C for 2 h. The white solids were filtered off and washed with hot water and methanol. Single crystals of the complex $[Eu(4\text{-iba})_3(H_2O)(dmf)]_2$ suitable for X-ray diffraction were obtained by slow diffusion of water into a dimethylformamide (dmf) solution of $[Eu(4\text{-iba})_3(H_2O)_2]$.

### Characterization

Unless otherwise indicated, all data were collected at a constant temperature of 298 $\pm$ 1 K. The chemical stoichiometries of the complexes were determined by $Ln^{3+}$ titration using a standard 0.01 mol $L^{-1}$ EDTA solution and elemental analysis of carbon and hydrogen (Perkin Elmer 2400). Thermogravimetric analysis (TA instruments SDTQ600) was carried out using a synthetic air flow (100 mL $min^{-1}$) at a heating rate of 10 °C $min^{-1}$. Infrared spectra (FT-IR Bomen FTLA 2000) data were obtained in transmission mode using KBr pellets. The diffuse reflectance spectra (DRS) of the europium(III) and gadolinium(III) complexes were obtained in the solid state in a Cary 5000 UV-Vis-NIR using $BaSO_4$ as the standard, using the absorption mode. The photoluminescence data were obtained with the samples in the solid state on a Fluorolog-3 spectrofluorometer (Horiba FL3-22-iHR320), with double-gratings (1200 gr $mm^{-1}$, 330 nm blazed) in the excitation monochromator and double-gratings (1200 gr $mm^{-1}$, 500 nm blazed) in the emission monochromator. An ozone-free xenon lamp of 450 W (Ushio) was used as a radiation source. The excitation spectra were obtained between 200 and 600 nm and they were corrected in real time according to the lamp intensity and the optical system of the excitation monochromator using a silicon diode as a reference detector. The emission spectra were obtained between 400 and 750 nm using the front face mode at 22.5°. All emission spectra were corrected according to the optical system of the emission monochromator and the photomultiplier response (Hamamatsu R928P). The time-resolved phosphorescence emission spectra of the analogous gadolinium(III) complexes were obtained at $\sim$77 K using a TCSPC system with successive delay increments, in order to get only the emissions from triplet levels of the ligands. The energy values of the ligand triplet level were obtained using two approaches: (i) fitting a tangent to the highest energy edge of the emission spectra or (ii) the maximum of the highest energy vibrational-coupled band (0–0 phonon) obtained from the deconvolution of the emission spectra.[15] The emission decay curves were obtained with a pulsed 150 W xenon lamp using a TCSPC system. The absolute quantum yields were measured using a Quanta-φ (Horiba F-309) integrating sphere equipped with an optical-fibers bundle (NA = 0.22 – Horiba-FL-3000/FM4-3000) using excitation centered in the f–f transitions due to the instrumental setup. The Judd–Ofelt (JO) intensity parameters ($\Omega_2$ and $\Omega_4$) and the efficiency parameters ($A_{rad}$, $A_{tot}$ and $\eta$) were calculated using the equations widely

 

described in the literature.[4] The number of coordinated water molecules ($q$) was determined using eqn (1), proposed by Horrocks *et al.* considering that the O–H oscillator is the only quenching route of the emitting level.[16]

$$q = A \cdot \left( \frac{1}{\tau_{H_2O}} - \frac{1}{\tau_{D_2O}} - \alpha \right) \quad (1)$$

where $A$ = 1.1, $\alpha$ = 0.31 and $\tau_{D_2O} = \tau_{rad}$ for Eu(III).[17]

### X-ray crystallographic characterization

Crystal data, data collection and refinement details for $[Eu(4\text{-iba})_3(H_2O)(dmf)]_2$ are given in Table 1. Eu–O bond lengths for this complex are shown in Table 2. A suitable crystal was mounted on a glass fiber and placed in the low-temperature nitrogen stream (Oxford Cryosystems 700 series). Data were collected on a Bruker APEX II DUO area detector diffractometer equipped with a low-temperature device, using graphite-monochromated Mo-Kα radiation ($\lambda$ = 0.71073 Å). Data were measured using a strategy combining $\omega$ and $\varphi$ scans of 0.3° per frame and an acquisition time of 10 s per frame. Multi-scan absorption corrections were applied. Cell parameters were retrieved using the SMART[18] software and refined using SAINT-Plus[19] on all observed reflections. Data reduction and correction for Lp and decay were performed using the SAINTPlus software.[19] Absorption corrections were applied using SADABS.[20] The structures were solved by direct methods and refined by least-squares methods on $F^2$ using the SHELXTL program package.[21] All non-hydrogen atoms were refined anisotropically. Almost all hydrogen atoms were added geometrically, and their parameters constrained to the parent site. The hydrogen atoms of the coordinated water molecule were located on the difference map. CCDC 1024660 contains the supplementary crystallographic data for $[Eu(4\text{-iba})_3(H_2O)(dmf)]_2$ in this paper.

### Ground state geometries and theoretical calculations

The Sparkle/PM3 model was used to determine the ground state geometries of the complexes.[22] In this model the lanthanide ion is replaced by a +3$e$ point charge.[23] The RHF wave functions were optimized using the Broyden–Fletcher–Goldfarb–Shanno (BFGS) procedure with a convergence criterion of 0.15 kcal mol$^{-1}$ Å$^{-1}$ and the semi empirical PM3 with a convergence criterion of $10^{-6}$ kcal mol$^{-1}$ for the SCF. In the Mopac2012 package[24] the following keywords were used: PM3, SPARKLE, XYZ, SCFCRT = 1D-10, GEO-OK, BFGS, CHARGE = X, PRECISE, GNORM = 0.15 and $T$ = 1D. The theoretical JO intensity parameters were calculated using the adequate equations and adjusting, in the physical acceptable range,[4] the polarizability ($\alpha$) and the charge factors ($g$) of the ligands in order to fit the theoretical JO intensity parameters with the experimental ones. The excited state calculations were performed using the ORCA software[25] using the INDO/S-CIS[26] with the lanthanide replaced by a +3$e$ point charge.[4,23] The transfer and back transfer energy rates from ligand triplet levels to $^5D_{1,0}$ europium(III) levels as well the theoretical quantum efficiency and quantum yield were calculated using the adequate kinetics equations described by Malta and co-workers[27–29] implemented in the LUMPAC software.[30]

Table 2 Eu–O bond distances [Å] in $[Eu(4\text{-iba})_3(H_2O)(dmf)]_2$

| Bond | $d$/Å | Bond | $d$/Å |
|---|---|---|---|
| Eu1–O5′ | 2.332(2) | Eu1–O6 | 2.407(2) |
| Eu1–O7 | 2.355(2) | Eu1–O3 | 2.449(2) |
| Eu1–O8 | 2.377(2) | Eu1–O2 | 2.525(2) |
| Eu1–O1 | 2.399(2) | Eu1–O4 | 2.545(2) |

Symmetry code: 2 − $x$, 1 − $y$, 1 − $z$.

## Results and discussion

X-ray quality single crystals of the complex $[Eu(4\text{-iba})_3(H_2O)(dmf)]_2$ were obtained by slow diffusion of water into a dmf solution of $[Eu(4\text{-iba})_3(H_2O)_2]$. It crystallizes in the monoclinic $P2_1/c$ space group, with two homobimetallic dimers in the unit cell. Details of the crystallographic characterization are summarized in Table 1 and selected bond distances are given in Table 2. The asymmetric unit contains one half of the molecule, with the other half being generated by inversion. Each of the two Eu centers binds to two bidentate 4-iba ligands, as well as one water and one dmf molecule; two additional 4-iba ligands which bridge the two metal centers, as shown in Fig. 2a, complete the coordination sphere with a coordination number of 8. The coordination polyhedron around the ions is best described by a bicapped trigonal prism, as shown in Fig. 2b, with O2 and O4 of the bidentate carboxylates as the capping atoms.

The Eu–O bond lengths (Table 2) are in the range 2.332(2)–2.545(2) Å, within that expected for this type of ligands,[6,31,32] with the shortest bond to a bridging oxygen atom. While bridging carboxylates are often found in a bridging bidentate mode, in which two oxygen atoms bind to one metal and one of them bridges between two metals, the oxygen atom O5 binds

Table 1 Details of the X-ray crystallographic characterization of $[Eu(4\text{-iba})_3(H_2O)(dmf)]_2$

| Formula | $C_{48}H_{42}Eu_2I_6N_4O_{16}$ | $T$/K | 100(2) |
|---|---|---|---|
| $M$/g mol$^{-1}$ | 1968.15 | $Z$ | 2 |
| Crystal system | Monoclinic | $D_c$/g cm$^{-3}$ | 2.258 |
| Space group | $P2_1/c$ | $\mu$(Mo-Kα)/mm$^{-1}$ | 5.411 |
| $a$/Å | 8.3983(8) | Independent reflections, $R_{int}$ [$F_o \geq 4\sigma(F_o)$] | 10 938; 0.0534 |
| $b$/Å | 25.310(3) | Reflections collected | 42 747 |
| $c$/Å | 14.1228(16) | $R_1$, w$R_2$ [$I > 2\sigma(I)$] | 0.0331; 0.0492 |
| $\alpha$/° | 90 | Data/restrains/parameters | 10 938/0/344 |
| $\beta$/° | 105.357(2) | GooF | 1.010 |
| $\gamma$/° | 90 | Largest diff. peak and hole/e Å$^{-3}$ | 1.229–0.900 |
| $V$/Å$^3$ | 2894.8(5) | | |

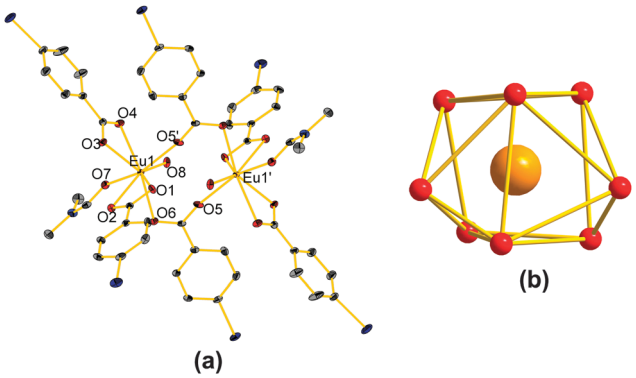


Fig. 2 (a) Plot of $[Eu(4\text{-iba})_3(H_2O)(dmf)]_2$ with thermal ellipsoids at 70% probability. Hydrogen atoms were omitted for clarity. (b) Bicapped trigonal prismatic coordination around the Eu(III).

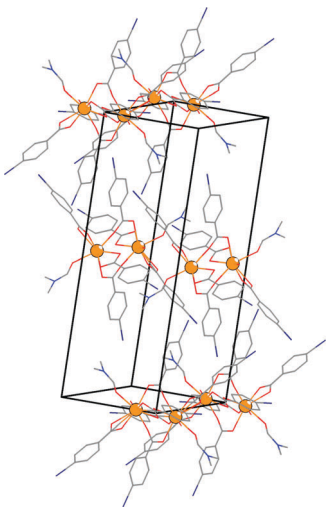

Fig. 3 Packing diagram of $[Eu(4\text{-iba})_3(H_2O)(dmf)]_2$.

only to Eu1', as its distance to Eu1 is 3.016(2) Å, which is longer than would be expected for a bonding interaction.[33]

Two dimers are present in the unit cell (see packing diagram in Fig. 3) with van der Waals interactions between the molecules and edge-to-face arrangement of the aromatic rings within the dimers and between adjacent molecules.

To date, no other X-ray quality single crystals were isolated and the remaining precipitated complexes were characterized in the powder form by TGA as well as FT-IR. The amount of non-coordinated (weight losses between 27 and 75 °C) and coordinated (weight losses between 75 and 200 °C) water molecules were determined by TGA analysis (Fig. S1–S4 and Table S2, ESI†). The coordination modes of the carboxylate group were determined by the calculation of $\Delta\nu$, where $\Delta\nu = \nu_a(COO^-) - \nu_s(COO^-)$. The FT-IR spectra (Fig. S6) and the coordination modes for each ligand (Table S3) are shown in the ESI.†

The triplet energy level (T) of the ligands was determined using the two approaches described in the Experimental section. The time resolved phosphorescence emission spectra of analogous gadolinium(III) complexes (Fig. S7) and the deconvolution of the phosphorescence bands (Fig. S8) are shown in the ESI.† The energy values of the triplet energy level obtained by the two approaches are shown in Table 3.

In order to explore the influence of the halogen at the *para* position of the benzoic acid on the luminescent properties of the europium(III) and terbium(III) complexes, the excitation (Fig. 4(A) and 5(A)) and the emission (Fig. 4(B) and 5(B)) spectra were obtained.

The excitation spectra of the complexes are composed of broad (assigned to the ligand transitions) and narrow bands (assigned to the 4f–4f transitions). For the majority of the complexes the intensities of the broad bands are higher than that of the narrow ones that might indicate energy transfer from the ligand to the lanthanide ion. The only exception of this case is for the complexes containing the 4-iba ligand. The absence of a broad band or a very low intensity one might be indicative of inefficient energy transfer from the 4-iba ligand to the lanthanide. The lower energy edge of the broad bands in the excitation spectra of the europium(III) complexes (Fig. 4(A)) seems to go towards lower energies from the 4-fba to the 4-iba ligands. That shift might be related to the presence of high energy LMCT states localized between the excited singlet and the triplet levels. The presence of LMCT states was investigated by the arithmetic difference between the diffuse reflectance spectra in the solid state of the europium(III) and gadolinium(III) complexes as performed by Carlos and co-workers.[34] The europium(III) and gadolinium(III) diffuse reflectance spectra of the complexes are shown in Fig. S9 (ESI†) and the resulting arithmetic difference between them is shown in Fig. 6.

The maxima of the LMCT bands are shifted towards lower energies from the 4-fba to 4-iba ligands and are in agreement with the redshift of the excitation bands edges. All LMCT bands have higher energy than the triplet state and they may transfer energy to the lanthanide ions, once they appear in the excitation spectra, or behave as intermediate states and transfer the energy to triplet levels.[35] The LMCT states can also work as deactivation channels if they have energy levels close or lower than the emission states as reported by Carlos and co-workers.[34] For terbium(III) compounds the presence of the LMCT states is more unlikely which can be observed by the narrowing of the excitation bands edges when compared with the europium(III) complexes (Fig. 5(A)) and also because of the lower $Tb^{3+} \rightarrow Tb^{2+}$ potential of reduction.[35]

The emission spectra of europium(III) complexes provide a lot of information about the point symmetry around the

Table 3 Energy of triplet levels of the ligands obtained by method (i) and (ii), described in the experimental section

| Complexes | $[Gd(4\text{-fba})_3(H_2O)_2]\cdot 1/2H_2O$ | $[Gd(4\text{-cba})_3(H_2O)]$ | $[Gd(4\text{-bba})_3(H_2O)_2]$ | $[Gd(4\text{-iba})_3(H_2O)_2]$ |
|---|---|---|---|---|
| $T^{(i)}/cm^{-1}$ | 26 765 | 24 704 | 25 485 | 21 789 |
| $T^{(ii)}/cm^{-1}$ | 26 035 | 23 299 | 23 811 | 20 736 |

 

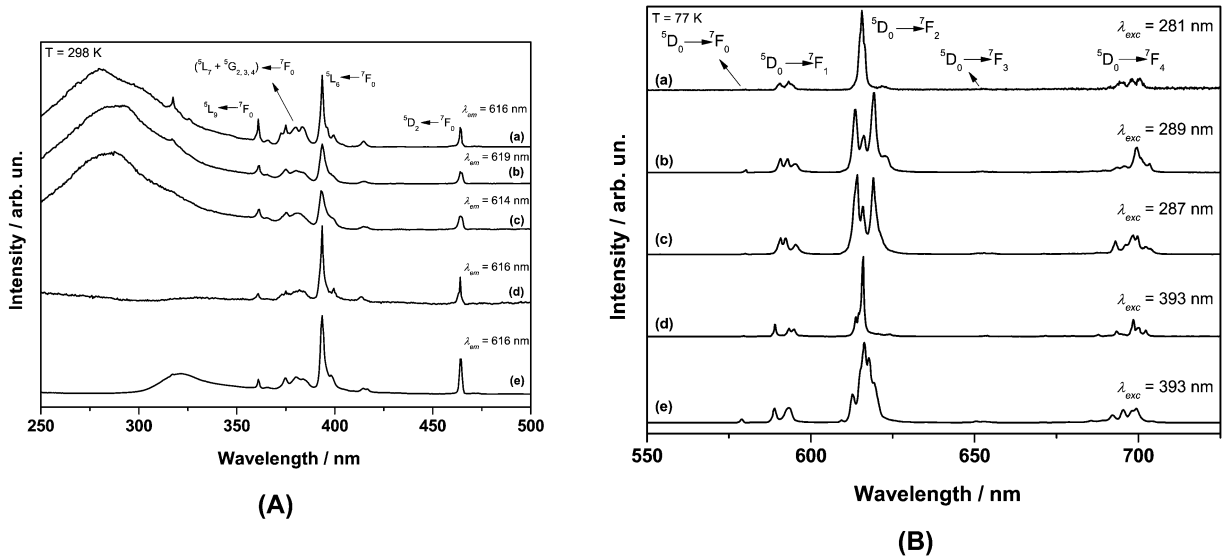


Fig. 4 (A) Excitation spectra of the europium(III) complexes obtained in the solid state. (B) Emission spectra of the europium(III) complexes obtained in the solid state. (a) $[Eu(4\text{-fba})_3(H_2O)_2]$. (b) $[Eu(4\text{-cba})_3]\cdot 2H_2O$. (c) $[Eu(4\text{-bba})_3]\cdot 5/2H_2O$. (d) $[Eu(4\text{-iba})_3(H_2O)_2]$. (e) $[Eu(4\text{-iba})_3(H_2O)(dmf)]_2$.

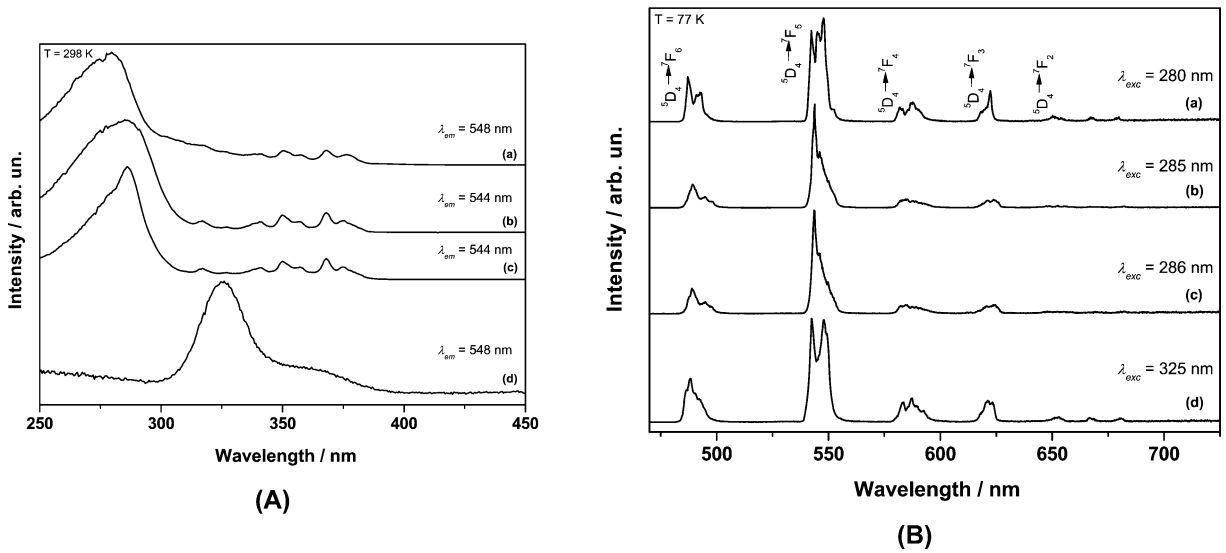


Fig. 5 (A) Excitation spectra of the terbium(III) complexes obtained in the solid state. (B) Emission spectra of the terbium(III) complexes obtained in the solid state. (a) $[Tb(4\text{-fba})_3(H_2O)_2]\cdot 1/2H_2O$. (b) $[Tb(4\text{-cba})_3(H_2O)_2]$. (c) $[Tb(4\text{-bba})_3(H_2O)]$. (d) $[Tb(4\text{-iba})_3(H_2O)_2]$.

europium(III) ion[36] and also about the covalence between Eu–L bonds.[37–39] For all emission spectra of europium(III) complexes, Fig. 4(B), the expected transitions $^5D_0 \rightarrow {}^7F_J$, ($J$ = 0; 1; 2; 3 and 4) are present. In addition, for all of them, the $^5D_0 \rightarrow {}^7F_2$ transition intensity is higher than $^5D_0 \rightarrow {}^7F_1$ ones, indicating that the forced electric dipole and the dynamic coupling mechanisms are predominant in relation to magnetic dipole ones because the europium(III) ion is located in a low symmetry site. The number of lines (splitting) of the europium(III) emission spectrum may be correlated with the point symmetry.[36] The complexes $[Eu(4\text{-cba})_3]\cdot 2H_2O$, $[Eu(4\text{-bba})_3]\cdot 5/2H_2O$ and $[Eu_2(4\text{-iba})_6(H_2O)_2(dmf)_2]$ show more splittings at ~77 K (Fig. 4B(b, c and e)), for each $^5D_0 \rightarrow {}^7F_J$ transition when compared with the $[Eu(4\text{-fba})_3(H_2O)_2]$ and $[Eu(4\text{-iba})_3(H_2O)_2]$ complexes, Fig. 4B(a and d). Therefore, the chemical environments around europium(III) ions in the $[Eu(4\text{-cba})_3]\cdot 2H_2O$, $[Eu(4\text{-bba})_3]\cdot 5/2H_2O$ and $[Eu_2(4\text{-iba})_6(H_2O)_2(dmf)_2]$ complexes are less symmetric than that of the $[Eu(4\text{-fba})_3(H_2O)_2]$ complex.

The energy of the $^5D_0 \rightarrow {}^7F_0$ transition can be correlated with the covalence degree of Eu–L bonds.[37–39] In order to build a comparative scale, high-resolution spectra for the $^5D_0 \rightarrow {}^7F_0$ transition were obtained, Fig. 7. The centroid energy of this transition was determined and the values are shown in Table 4.

The values of the $^5D_0 \rightarrow {}^7F_0$ energy are virtually the same. That means that the changes of the halogen at the *para* position do not cause significant changes in the covalence between Eu–O (carboxylate) bonds. It is important to point out that the $^5D_0 \rightarrow {}^7F_0$ emission spectrum of the $[Eu(4\text{-iba})_3(H_2O)_2]$

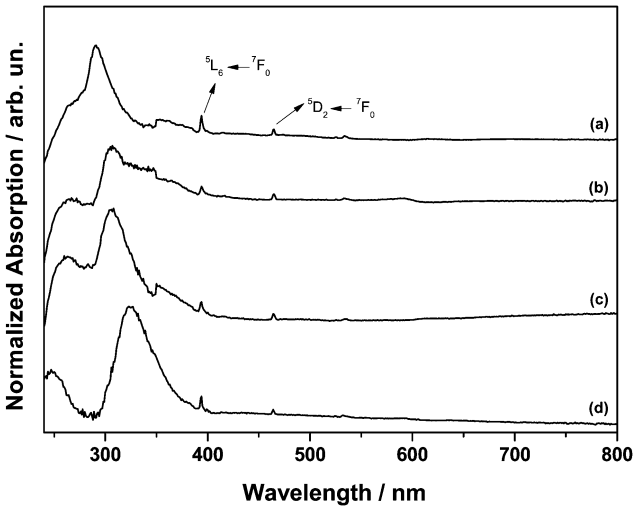


Fig. 6 Arithmetic difference between the europium(III) and gadolinium(III) diffuse reflectance spectra showing the LMCT bands; (a) 4-fba. (b) 4-cba. (c) 4-bba. (d) 4-iba.

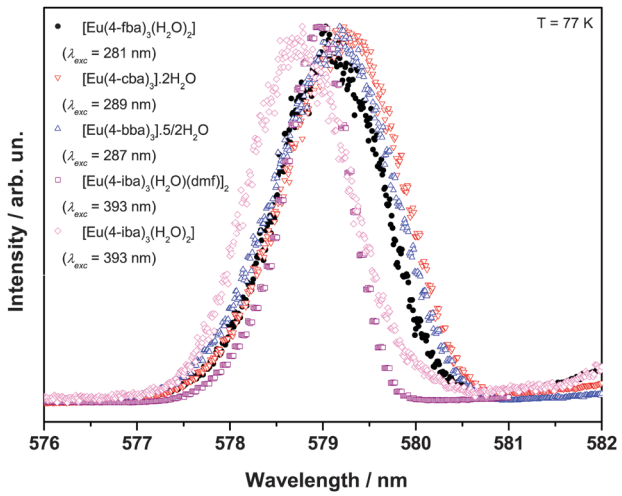


Fig. 7 High-resolution spectra of the $^5D_0 \rightarrow {}^7F_0$ transition of the europium(III) complexes; black dot: [Eu(4-fba)$_3$(H$_2$O)$_2$], red down triangle: [Eu(4-cba)$_3$]·2H$_2$O, blue up triangle: [Eu(4-bba)$_3$]·5/2H$_2$O, purple square: [Eu(4-iba)$_3$(H$_2$O)(dmf)]$_2$ and light magenta rhomb: [Eu(4-iba)$_3$(H$_2$O)$_2$].

Table 4 Energy of the $^5D_0 \rightarrow {}^7F_0$ transition of the europium(III) complexes

| Complexes | $E_{00}$/cm$^{-1}$ |
|---|---|
| [Eu(bza)$_3$(H$_2$O)][40] | 17 270 |
| [Eu(4-fba)$_3$(H$_2$O)$_2$] | 17 270 |
| [Eu(4-cba)$_3$(H$_2$O)$_2$]·2H$_2$O | 17 266 |
| [Eu(4-bba)$_3$]·5/2H$_2$O | 17 269 |
| [Eu(4-iba)$_3$(H$_2$O)$_2$] | 17 278 |
| [Eu(4-iba)$_3$(H$_2$O)(dmf)]$_2$ | 17 275 |

(powder) complex is broader than that of the [Eu(4-iba)$_3$(H$_2$O)(dmf)]$_2$ (single crystal), probably due to the less homogeneity of the europium(III) sites in the powder ([Eu(4-iba)$_3$(H$_2$O)$_2$]) when compared with the single crystal ([Eu(4-iba)$_3$(H$_2$O)(dmf)]$_2$). However, this broadening or the insertion of the dmf ligand in the coordination sphere does not cause significant changes in the covalence degree of the Eu–O bonds (Table 4).

Table 5 Judd–Ofelt intensity parameters ($\Omega_2$ and $\Omega_4$), radiative rate ($A_{rad}$), and quantum efficiency ($\eta$) for europium(III) complexes

| Complexes | $\Omega_2/10^{-20}$ cm$^2$ | $\Omega_4/10^{-20}$ cm$^2$ | $A_{rad}$/s$^{-1}$ | $\eta$/% |
|---|---|---|---|---|
| [Eu(4-fba)$_3$(H$_2$O)$_2$] | 10.4 | 9.0 | 496 | 23 |
| [Eu(4-cba)$_3$]·2H$_2$O | 10.0 | 5.4 | 461 | 46 |
| [Eu(4-bba)$_3$]·5/2H$_2$O | 11.5 | 7.6 | 506 | 52 |
| [Eu(4-iba)$_3$(H$_2$O)$_2$] | 8.9 | 8.4 | 441 | 19 |
| [Eu(4-iba)$_3$(H$_2$O)(dmf)]$_2$ | 13.4 | 5.5 | 532 | 24 |

In order to get a better insight about the point symmetry around the europium(III) ion the Judd–Ofelt intensity parameters[41,42] were obtained, Table 5. The equations used to obtain these parameters are widely discussed in the literature.[4,43,44]

The JO intensity parameters $\Omega_2$ and $\Omega_4$ are strongly correlated with the point symmetry around the europium(III) ion. A high value for the $\Omega_2$ intensity parameter means a low point symmetry around the europium(III) ion. For this series, the complexes [Eu(4-cba)$_3$]·2H$_2$O, [Eu(4-bba)$_3$]·5/2H$_2$O and [Eu(4-iba)$_3$(H$_2$O)(dmf)]$_2$ show the highest values for the $\Omega_2$ intensity parameter that means the europium ion lies in a lower symmetry site in these complexes when compared with the [Eu(4-fba)$_3$(H$_2$O)$_2$] and [Eu(4-iba)$_3$(H$_2$O)(dmf)]$_2$ complexes. These conclusions match well with the observations done for the emission spectra where the [Eu(4-cba)$_3$]·2H$_2$O, [Eu(4-bba)$_3$]·5/2H$_2$O and [Eu(4-iba)$_3$(H$_2$O)(dmf)]$_2$ complexes show a similar emission profile regarding the splitting of the $^5D_0 \rightarrow {}^7F_J$ transitions.

The Horrock's equation[16] (eqn (1)) can be used for the determination of coordinated water molecules when the O–H oscillators are the only non-radiative route for de-activation of the emitting level of the lanthanide(III). The values obtained by the Horrock's equation[16] ($q^a$) (Table 6) are very close to the ones determined by TGA ($q^b$) (Table S2, ESI†). The good agreement between the values obtained (Table 6) confirms the absence of additional de-activation routes, such as low energy LMCT states.

All emission decay curves of the $^5D_0$ (europium(III)) and $^5D_4$ (terbium(III)) emitting levels were fitted as a mono exponential decay (Fig. S10, ESI†) and the values obtained for the emission lifetime ($\tau$) are shown in Table 7. It is well known that for europium(III) ions there is a strong correlation between the lifetime and the non-radiative processes such as O–H and N–H oscillators.[2] As expected the highest lifetime values were obtained for the [Eu(4-cba)$_3$]·2H$_2$O and [Eu(4-bba)$_3$]·5/2H$_2$O complexes due to the absence of water in the first coordination sphere.

Table 6 Number of coordinated water molecules obtained by the Horrocks equation[16] ($q^a$) and by TGA ($q^b$)

| Complexes | $q^a$ | $q^b$ |
|---|---|---|
| [Eu(4-fba)$_3$(H$_2$O)$_2$] | 2.4 | 2 |
| [Eu(4-cba)$_3$]·2H$_2$O | 0.24 | 0 |
| [Eu(4-bba)$_3$]·5/2H$_2$O | 0.18 | 0 |
| [Eu(4-iba)$_3$(H$_2$O)$_2$] | 1.8 | 2.0 |
| [Eu(4-iba)$_3$(H$_2$O)(dmf)]$_2$ | 1.5 | 2.0[a] |

[a] Coordinated water molecules obtained from crystal data of homobimetallic (Fig. 2a).

 

Table 7 Values of lifetimes ($\tau$) and absolute quantum yield obtained for the complexes (all the values of the absolute quantum yield were obtained with excitation centered in $^5D_2 \leftarrow {}^7F_0$, for europium(III), or $^5L_{10} \leftarrow {}^7F_6$, for terbium(III), transitions)

| Complexes | $\Phi_{Eu}^{Eu}$/% | $\tau$/ms | Complexes | $\Phi_{Tb}^{Tb}$/% | $\tau$/ms |
|---|---|---|---|---|---|
| $[Eu(4\text{-fba})_3(H_2O)_2]$ | 4 ± 1 | 0.421 ± 0.002 | $[Tb(4\text{-fba})_3(H_2O)]\cdot 1/2(H_2O)$ | 4.5 ± 0.2 | 0.966 ± 0.003 |
| $[Eu(4\text{-cba})_3]\cdot 2H_2O$ | 19 ± 1 | 1.006 ± 0.007 | $[Tb(4\text{-cba})_3(H_2O)_2]$ | 14 ± 1 | 0.888 ± 0.004 |
| $[Eu(4\text{-bba})_3]\cdot 5/2H_2O$ | 18 ± 1 | 1.02 ± 0.02 | $[Tb(4\text{-bba})_3(H_2O)]$ | 2.4 ± 0.3 | 0.623 ± 0.006 |
| $[Eu(4\text{-iba})_3(H_2O)_2]$ | 4 ± 1 | 0.503 ± 0.001 | $[Tb(4\text{-iba})_3(H_2O)_2]$ | <1 | 0.80 ± 0.01 |
| $[Eu(4\text{-iba})_3(H_2O)(dmf)]_2$ | 8 ± 1 | 0.458 ± 0.002 | — | — | — |

The emission lifetime values for the $[Eu(4\text{-fba})_3(H_2O)_2]$, $[Eu(4\text{-iba})_3(H_2O)(dmf)]_2$ and $[Eu(4\text{-iba})_3(H_2O)_2]$ complexes are similar to each other and lower than the values obtained for the $[Eu(4\text{-cba})_3]\cdot 2H_2O$ and $[Eu(4\text{-bba})_3]\cdot 5/2H_2O$ complexes due to the presence of water in the first coordination sphere. For terbium(III) compounds there is no strong correlation between the lifetime and the non-radiative processes due to the higher energy gap between the fundamental and excited levels, when compared with europium(III) ions. One can see, in Table 7, that the terbium(III) complexes show nearly the same emission lifetime values, the one for $[Tb(4\text{-bba})_3(H_2O)]$ being the smallest.

The absolute quantum yield values of the complexes (Table 7) were obtained in the solid state with the excitation centered in the $^5D_2 \leftarrow {}^7F_0$ (~396 nm) transition of the europium(III) ion or in the $^5L_{10} \leftarrow {}^7F_6$ (~368 nm) transition of the terbium(III) ion. In this case the absolute quantum yields cannot be correlated with the ligand properties because they were obtained with excitation centered in the metal bands due to the instrumental limitations. Once the excitation was centered in the 4f–4f transitions one should expect a quantum yield strongly correlated with the non-radiative processes, such as vibronic coupling with O–H oscillators or back energy transfer from europium(III) or terbium(III) to ligand levels. The highest values were obtained for the $[Eu(4\text{-cba})_3]\cdot 2H_2O$ and $[Eu(4\text{-bba})_3]\cdot 5/2H_2O$ complexes probably because of the absence of coordinated water molecules, once the energy value of the triplet levels of the ligands are similar (Table 3) and the back energy transfer rates do not play an important role in these series of complexes (Table 9). As expected, the presence of coordinated water molecules plays an important role in the quantum yield in this series.

To get a better insight about the energy transfer rates, the ground state geometries of the europium(III) complexes were determined using the Sparkle/PM3[22] model implemented in the MOPAC2012 software[24] and are shown in Fig. S11 (ESI†). In order to keep rigid the central polyhedron, the strategy to calculate the ground state geometries was based on the methodology used by Freire and co-workers[45] and Sigoli and co-workers[40] for dimers or polymers: three metallic centers were drawn, the central metal is coordinated by different modes: bidentate bridge and/or bidenate chelate and/or bidentate bridging and chelate simultaneously, the two other metallic centers have only the function to keep the structure rigid and the coordination sphere was filled with water molecules, Fig. 8. The oxygen atoms, directly bonded to the europium(III) ion, were also divided into groups in order to obtain the polarizability ($\alpha$) and charge factor ($g$) values, Fig. 9.

The theoretical JO intensity parameters were obtained by adjusting the polarizability ($\alpha$) and charge factor ($g$) in order to match the experimental JO intensity parameter values. The oxygen atoms were divided into 4 groups: (i) oxygens that bond exclusively by the bidentate bridging mode (group 1); (ii) oxygens that simultaneously bond by the bidentate bridging and chelate mode (group 2A and 2B); (iii) oxygens that bond exclusively by the bidentate chelate mode (group 3) and (iv) oxygens from water molecules (group 4). The values obtained for polarizability ($\alpha$) and charge factor ($g$) are shown in the ESI† (Table S3).

The values obtained for the theoretical JO intensity parameters are shown in Table 8 and compared with the experimental ones.

There is good agreement between the experimental and calculated JO intensity parameters except for the case of the $\Omega_4$ intensity parameter in the $[Eu(4\text{-bba})_3]\cdot 5/2H_2O$ complex. The poor agreement between the calculated and experimental JO intensity parameters might be due to the approximated propositions of the coordination polyhedron of carboxylate

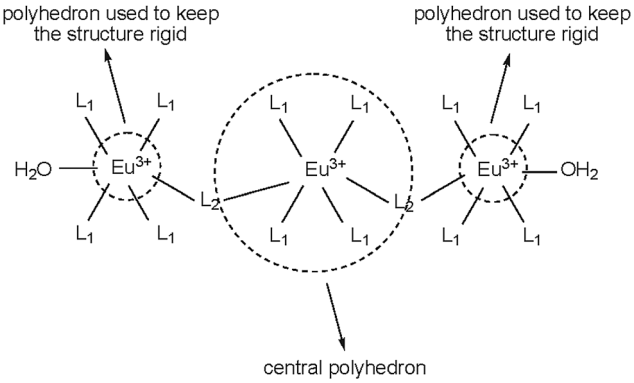


Fig. 8 Strategy used to simulate the structure of the complexes.

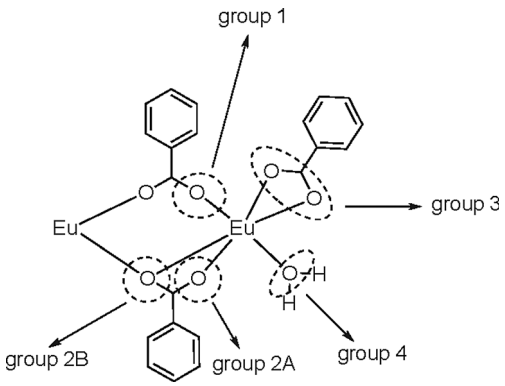


Fig. 9 Division of the oxygen atoms into groups for calculation of the polarizability and charge factors.

Table 8 Calculated and experimental JO intensity parameters. In parentheses the data obtained using single crystals

| Complexes | $(\Omega_2)_{theo}/10^{-20}$ cm$^2$ | $(\Omega_2)_{exp}/10^{-20}$ cm$^2$ | $(\Omega_4)_{theo}/10^{-20}$ cm$^2$ | $(\Omega_4)_{exp}/10^{-20}$ cm$^2$ | $(\Omega_6)_{theo}/10^{-20}$ cm$^2$ |
|---|---|---|---|---|---|
| $[Eu(4\text{-fba})_3(H_2O)_2]$ | 10.4 | 10.4 | 9.0 | 8.4 | 0.26 |
| $[Eu(4\text{-cba})_3]\cdot 2(H_2O)$ | 11.7 | 11.0 | 4.0 | 5.4 | 0.42 |
| $[Eu(4\text{-bba})_3]\cdot 5/2H_2O$ | 12.1 | 11.5 | 1.4 | 7.6 | 0.53 |
| $[Eu(4\text{-iba})_3(H_2O)_2]$ | 8.9 | 8.9 | 8.4 | 8.4 | 0.26 |
| $[Eu(4\text{-iba})_3(H_2O)(dmf)]_2$ | 13.4 (13.4) | 13.4 | 5.5 (5.5) | 5.5 | 0.13 (0.17) |

Table 9 Energy transfer and back transfer rates between the ligand triplet level and $^5D_1$ and $^5D_0$ europium(III) levels, calculated from the ground state geometries provided by Sparkle/PM3

| Complexes | T → $^5D_1$ | $^5D_1$ → T | T → $^5D_0$ | $^5D_0$ → T | $R_L$/Å |
|---|---|---|---|---|---|
| $[Eu(4\text{-fba})_3(H_2O)_2]$ | $1.5 \times 10^4$ | $1.8 \times 10^{-10}$ | $5.0 \times 10^3$ | $1.2 \times 10^{-14}$ | 6.2057 |
| $[Eu(4\text{-cba})_3]\cdot 2(H_2O)$ | $1.4 \times 10^6$ | $6.3 \times 10^{-3}$ | $8.6 \times 10^5$ | $7.9 \times 10^{-7}$ | 5.6366 |
| $[Eu(4\text{-bba})_3]\cdot 5/2H_2O$ | $2.1 \times 10^5$ | $2.6 \times 10^{-8}$ | $7.9 \times 10^4$ | $2.0 \times 10^{-12}$ | 5.7297 |

Table 10 Theoretical and experimental quantum efficiencies ($\eta$) and quantum yields ($\Phi$)

| Complexes | $\eta_{theo}$/% | $\eta_{exp}$/% | $\Phi_{theo}$/% |
|---|---|---|---|
| $[Eu(4\text{-fba})_3(H_2O)_2]$ | 21 | 23 | 1 |
| $[Eu(4\text{-cba})_3]\cdot 2(H_2O)$ | 35 | 46 | 24 |
| $[Eu(4\text{-bba})_3]\cdot 5/2H_2O$ | 44 | 52 | 10 |

groups coordinated. Also, in this case intermolecular interactions might play an important role for the structure.

The energy transfer rates (Table 9) were calculated for all complexes except for the $[Eu_2(4\text{-iba})_6(H_2O)_2]$ and the $[Eu(4\text{-iba})_3(H_2O)(dmf)]_2$ complexes due to the absence of parameters for the iodine atom in the ORCA software.[25] For all complexes the energy transfer, from the ligand to the lanthanide, is higher than the back transfer ones. The highest energy transfer rates, from the ligand to the lanthanide, were obtained for the $[Eu(4\text{-cba})_3]\cdot 2H_2O$ complex which might be due to the smaller value of the $R_L$ parameter. The values obtained for the transfer rates are smaller than the ones obtained for other systems like tris β-diketonates.[46]

The quantum efficiency and quantum yield values were obtained using adequate kinetics equations[27–29] and are shown in Table 10. The values obtained using the Sparkle/PM3[22] ground state geometries are in good agreement with the experimental ones.

As expected the anhydrous complex shows higher values for, both, theoretical quantum efficiency and quantum yield. The high quantum yield of the $[Eu(4\text{-cba})_3]\cdot 2H_2O$ complex is due to the combination of absence of coordinated solvent molecules and also the low value of the back transfer energy from the $^5D_{1,0}$ to the ligand triplet levels, Table 10.

## Conclusions

The rich coordination modes of the ligands containing the carboxylate group provide a very interesting system for photophysical studies. The influence of the halogen on the photophysical properties was verified by photoluminescence spectroscopy. The point symmetries of the complexes were compared using the splittings of each $^5D_0 \rightarrow {}^7F_J$ and the JO intensity parameters. It was found that there is a similar symmetry occupied by the europium(III) ion in the complexes $[Eu(4\text{-cba})_3]\cdot 2H_2O$, $[Eu(4\text{-bba})_3]\cdot 5/2H_2O$ and $[Eu(4\text{-iba})_3(H_2O)(dmf)]_2$. A comparative covalence degree of the Eu–O bonds was obtained by the energy of the $^5D_0 \rightarrow {}^7F_0$ transition. In this series the different halogens (F, Cl, Br and I) at the *para* position and the solvent molecule do not change the degree of covalence for the Eu–O bonds significantly. The presence of LMCT states was confirmed by the arithmetic subtraction between the diffuse reflectance spectra of europium(III) and gadolinium(III) and the energy of the LMCT state decreases from the 4-fba to the 4-iba ligand. The highest emission lifetimes and quantum yields were obtained for the $[Eu(4\text{-cba})_3]\cdot 2H_2O$ and $[Eu(4\text{-bba})_3]\cdot 5/2H_2O$ complexes due to the absence of coordinated water molecules.

Therefore, the halogen change at the *para* position of the aromatic ring of the benzoic acid does change both molecular structure and photophysical properties. The experimental observations done in this work will help the design of new luminescent compounds with desirable properties and also as data for understanding the influence of the modifications in the ligand structure and the changes in the photophysical properties.

## Acknowledgements

JHSKM is indebted to CNPq for a PhD fellowship. AdBD acknowledges NSF (grant CHE 1363325) for financial support. FAS and IOM are indebted to CNPq, CAPES and FAPESP (Grant no. 2008/53868-0) for financial support. The authors would like to thank the Laboratory of Advanced Optical Spectroscopy (LMEOA/IQ-UNICAMP/FAPESP Grant no. 2009/54066-7). This work is a contribution of the National Institute of Science and Technology in Complex Functional Materials (CNPq-MCT/FAPESP).

## References

1 K. Binnemans, *Chem. Rev.*, 2007, **107**, 2592–2614.
2 J.-C. G. Bünzli and S. V. Eliseeva, in *Lanthanide Luminescence: Photophysical, Analytical and Biological Aspects*, ed. P. Hänninen and H. Härmä, Springer, Berlin, 2011, ch. 1, pp. 1–46.
3 J.-C. G. Bünzli, *Chem. Rev.*, 2010, **110**, 2729–2755.

 

4 G. F. de Sá, O. L. Malta, C. de Mello Donegá, A. M. Simas, R. L. Longo, P. A. Santa-Cruz and E. F. da Silva Jr, *Coord. Chem. Rev.*, 2000, **196**, 165–195.
5 G. B. Deacon and R. J. Phillips, *Coord. Chem. Rev.*, 1980, **33**, 227–250.
6 X. Li, Z.-Y. Zhang and Y.-Q. Zou, *Eur. J. Inorg. Chem.*, 2005, 2909–2918.
7 L.-J. Xu, S.-P. Wang, R.-F. Wang and J.-J. Zhang, *J. Coord. Chem.*, 2008, **61**, 237–250.
8 B. S. Zhang, *Acta Crystallogr., Sect. E: Struct. Rep. Online*, 2006, **62**, M2645–M2647.
9 X. Li, T.-T. Zhang, Y.-L. Ju, C.-Y. Wang, Y.-Q. Li, L. Zhang and Q. Zhang, *J. Coord. Chem.*, 2007, **60**, 2121–2132.
10 H.-Y. Zhang, J.-J. Zhang, N. Ren, S.-L. Xu, L. Tian and J.-H. Bai, *J. Alloys Compd.*, 2008, **464**, 277–281.
11 X. Li, Y.-L. Ju and Y.-Q. Zou, *J. Coord. Chem.*, 2007, **60**, 1513–1526.
12 A. P. Souza, L. C. V. Rodrigues, H. F. Brito, S. Alves Jr and O. L. Malta, *J. Lumin.*, 2010, **130**, 181–189.
13 S. K. Lower and M. A. El-Sayed, *Chem. Rev.*, 1966, **66**, 199–241.
14 M. Hilder, P. C. Junk, U. H. Kynast and M. M. Lezhnina, *J. Photochem. Photobiol., A*, 2009, **202**, 10–20.
15 G. A. Crosby, R. E. Whan and R. M. Alire, *J. Chem. Phys.*, 1961, **34**, 743.
16 R. M. Supkowski and W. D. Horrocks, *Inorg. Chim. Acta*, 2002, **340**, 44–48.
17 L. D. Carlos, R. A. Ferreira, Z. Bermudez Vde and S. J. Ribeiro, *Adv. Mater.*, 2009, **21**, 509–534.
18 *SMART: Bruker Molecular Analysis Research Tool*, Bruker, v.5.626 edn, 2002.
19 *SAINTPlus: Data Reduction and Correction Program*, v.6.36a edn, 2001.
20 *SADABS: an Empirical Absorption Correction Program*, v. 2.01 edn, 2001.
21 G. M. Sheldrick, v.6.10 edn, 2001.
22 R. O. Freire, G. B. Rocha and A. M. Simas, *J. Braz. Chem. Soc.*, 2009, **20**, 1638–1645.
23 A. V. M. Andrade, N. B. Costa, A. M. Simas and G. F. de Sá, *Chem. Phys. Lett.*, 1994, **227**, 349–353.
24 J. J. P. Stewart, *Stewart Computational Chemistry*, Colorado Springs, 2012.
25 F. Neese, *Wiley Interdiscip. Rev.: Comput. Mol. Sci.*, 2012, **2**, 73–78.
26 J. E. Ridley and M. C. Zerner, *Theor. Chim. Acta*, 1976, **42**, 223–236.
27 O. L. Malta, *J. Lumin.*, 1997, **71**, 229–236.
28 F. R. G. Silva and O. L. Malta, *J. Alloys Compd.*, 1997, **250**, 427–430.
29 O. L. Malta, *J. Non-Cryst. Solids*, 2008, **354**, 4770–4776.
30 J. D. Dutra, T. D. Bispo and R. O. Freire, *J. Comput. Chem.*, 2014, **35**, 772–775.
31 F. Cagnin, M. R. Davolos and E. E. Castellano, *Polyhedron*, 2014, **67**, 65–72.
32 E. R. Souza, I. O. Mazali and F. A. Sigoli, *J. Fluoresc.*, 2014, **24**, 203–211.
33 S. Viswanathan and A. de Bettencourt-Dias, *Inorg. Chem.*, 2006, **45**, 10138–10146.
34 J. A. Fernandes, R. A. S. Ferreira, M. Pillinger, L. D. Carlos, I. S. Goncalves and P. J. A. Ribeiro-Claro, *Eur. J. Inorg. Chem.*, 2004, 3913–3919, DOI: 10.1002/ejic.200400191.
35 J.-C. G. Bünzli, *Coord. Chem. Rev.*, DOI: 10.1016/j.ccr.2014.10.013.
36 P. A. Tanner, in *Lanthanide Luminescence: Photophysical, Analytical and Biological Aspects*, ed. P. Hänninen and H. Härmä, Springer, Berlin, 2011, ch. 7, pp. 183–233.
37 S. T. Frey and W. D. Horrocks, *Inorg. Chim. Acta*, 1995, **229**, 383–390.
38 L. D. Carlos, O. L. Malta and R. Q. Albuquerque, *Chem. Phys. Lett.*, 2005, **415**, 238–242.
39 O. L. Malta, H. J. Batista and L. D. Carlos, *Chem. Phys.*, 2002, **282**, 21–30.
40 J. H. S. K. Monteiro, A. L. B. Formiga and F. A. Sigoli, *J. Lumin.*, 2014, **154**, 22–31.
41 B. R. Judd, *Phys. Rev.*, 1962, **127**, 750–761.
42 G. S. Ofelt, *J. Chem. Phys.*, 1962, **37**, 511–520.
43 O. L. Malta, *Chem. Phys. Lett.*, 1982, **87**, 27–29.
44 O. L. Malta, M. A. C. dos Santos, L. C. Thompson and N. K. Ito, *J. Lumin.*, 1996, **69**, 77–84.
45 M. O. Rodrigues, N. B. da Costa Jr., C. A. de Simone, A. A. S. Araujo, A. M. Brito-Silva, F. A. A. Paz, M. E. de Mesquita, S. A. Junior and R. O. Freire, *J. Phys. Chem. B*, 2008, **112**, 4204–4212.
46 J. H. S. K. Monteiro, R. D. Adati, M. R. Davolos, J. R. M. Vicenti and R. A. Burrow, *New J. Chem.*, 2011, **35**, 1234.